Journal of Engineering Physics and Thermophysics, Vol. 75, No. 6, 2002

MATHEMATICAL MODEL FOR CALCULATING THE HEAT-PROTECTION PROPERTIES OF THE COMPOSITE COATING "CERAMIC MICROSPHERES–BINDER"

M. L. German and P. S. Grinchuk UDC 536.33

A mathematical model which makes it possible to calculate the heat-protection properties of the composite coating "ceramic microspheres–binder" is proposed. The model takes account of the optical and thermophysical properties of the components and the optical properties of a substrate. It is shown that the decrease in the heat loss due to suppression of its radiative component by the coating in question can reach more than 50%. Under certain conditions, the heat-insulation effect can be absent or even inverted, i.e., the presence of the coating is capable of resulting in an increase in the heat flux from the surface being protected. Comparison of the data of the performed full-scale experiment and the calculations based on the proposed model showed that the latter adequately reflects the actual process of heat transfer and can be used for calculating the heat-protection properties of coatings representing a compound of a binder and ceramic microspheres.

Introduction. In a number of countries, for additional heat protection of buildings of various functional purposes one currently uses a coating consisting of hollow or dense ceramic (or glass) microspheres with a characteristic dimension of the order of 10–50 μm which are mixed with acryl paint. When dried, the coating has a thickness of the order of 0.3 mm and consists of several rows of microspheres bonded by a thin acryl film. The coating is characterized by a simple technique of deposition and, as reported by the producers, enables one to decrease the heat loss by no less than 30% and shows a rather high vapor permeability and low wettability. However, the problem on the influence of specific properties of the coating and the substrate on the efficiency of heat insulation remains to be solved.

Mathematical Formulation of the Problem of Radiative-Conductive Heat Transfer in the Layer of a Compound Consisting of Hollow Ceramic Microspheres and a Binder. We consider a compound layer of thickness H consisting of a binder and hollow ceramic microspheres and deposited on the external surface of a certain wall (Fig. 1).

The heat loss from the compound surface involves conductive, convective (loss due to the washing of the surface by the surrounding air), and radiative (due to the light exchange of the wall with the ground surface and the sky) components. Just the value of the heat flux from the coating surface and not the temperature of the latter can be used as the efficiency criterion of the heat-protection coating. Let the external surface of the considered wall have temperature T_w and a hemispherical emissivity ε_w. We will consider that the given quantities are as follows: 1) temperature of the surrounding air T_a; 2) temperature of the ground surface T_g and $T_g = T_a$; 3) effective radiative temperature of the sky T_r. When the weather is cloudy, T_r of the night sky is set to be 250 K, and when the sky is clear T_r = 100 K [1]. The hemispherical emissivity of the surrounding atmosphere is assumed to be equal to $\varepsilon_a = 1$. In the absence of the compound layer, the density of the heat-loss flux from the wall surface is determined by the loss due to convection and heat radiation [1]:

$$q_0 = q_{0\text{conv}} + q_{0\text{r}} = \alpha\,(T_w - T_a) + \varepsilon_w \sigma_* \,(T_w^4 - T_{\text{r.g}}^4)\,, \tag{1}$$

where σ_* is the Stefan–Boltzmann constant and $T_{\text{r.g}}^4 = (T_g^4 + T_r^4)/2$, $T_{\text{r.g}}$ being the mean radiative temperature of the surrounding medium. In the absence of wind, i.e., for the free-convection regime, the coefficient of convective heat transfer from the surface can be calculated according to the following formula [2]:

A. V. Luikov Heat and Mass Transfer Institute, National Academy of Sciences of Belarus, Minsk, Belarus. Translated from Inzhenerno-Fizicheskii Zhurnal, Vol. 75, No. 6, pp. 43–53, November–December, 2002. Original article submitted May 22, 2002.

1062-0125/02/7506-1301$27.00

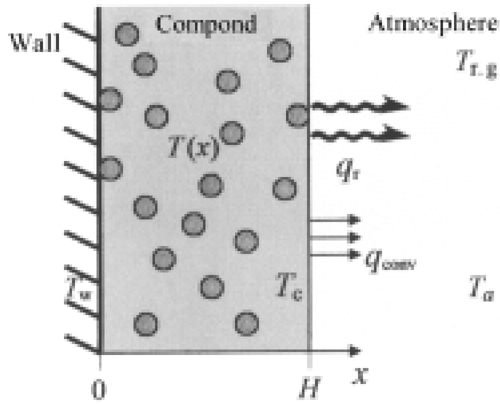

Fig. 1. Scheme of calculating the thermal regime of a compound layer.

$$\alpha = \frac{\lambda'_a}{L}\left[0.825 + \frac{0.38\,\mathrm{Ra}^{1/6}}{[1 + (0.492/\mathrm{Pr})^{9/16}]^{8/27}}\right]^2 , \tag{2}$$

where Ra = Pr Gr is the Rayleigh criterion expressed by the Grashof number $\mathrm{Gr} = g\beta_V L^3 (T_w - T_a)/\nu_a^2$ and the Prandtl number $\mathrm{Pr} = \nu_a / a'_a$. Here λ'_a, ν_a, and a'_a are the conductivity, kinematic viscosity, and thermal diffusivity of air respectively, which are determined from the tables [2] for the mean air temperature at the wall $\langle T \rangle = (T_w + T_a)/2$ and $\beta_V = 1/\langle T \rangle$ is the coefficient of volumetric expansion.

To account for the influence of the compound layer on the value of the heat loss from the wall surface, it is necessary to know the temperature distribution in the compound and the parameters characterizing the radiation transfer in it.

In the steady-state case, the temperature field in the compound layer is determined by the one-dimensional (by virtue of the small thickness of the layer) energy equation [3]

$$\lambda'_c \frac{d^2 T(x)}{dx^2} = \mathrm{div}\, \mathbf{Q}_r(x) , \quad x \in [0, H] . \tag{3}$$

Here div $\mathbf{Q}_r$ is the density of volumetric radiative heat sources in the compound layer. The boundary conditions for (3) reflect the special features of heat exchange on each layer surface. As a result of tight sticking of the compound to the wall, on the surface adjacent to the wall ($x = 0$) we have

$$T(0) = T_w . \tag{4}$$

By virtue of the fact that the compound is semitransparent to infrared (IR) radiation and the radiative flux on its surface is formed by both the internal layers and the heat radiation of the wall surface (i.e., radiative heat transfer occurs simultaneously with conductive heat transfer and their mutual influence is determined by the value of div $\mathbf{Q}_r(x)$), on the opposite side of the layer ($x = H$), we prescribe only the density of the convective heat flux:

$$q_{\mathrm{conv}} = -\lambda'_c \left.\frac{dT}{dx}\right|_{x=H} = \alpha\,(T\big|_{x=H} - T_a) . \tag{5}$$

The density of the radiation sources div $\mathbf{Q}_r(x)$ is determined by solution of the radiation-transfer equation which under the condition of local thermodynamic equilibrium has the form [4]

$$\mu \frac{dI_\lambda(x, \mu)}{dx} + (\chi_\lambda + \sigma_\lambda)\, I_\lambda(x, \mu) = \chi_\lambda B_\lambda(T) + \frac{\sigma_\lambda}{2} \int_{-1}^{1} p_\lambda(\mu, \mu')\, I_\lambda(x, \mu')\, d\mu' , \tag{6}$$

where $B_\lambda(T) = \dfrac{c_1 n_1^2}{\pi\lambda^5(\exp(c_2/\lambda T) - 1)}$ is the spectral intensity of radiation of the ideal black body at temperature T in the binder medium with a refractive index of $m_b = n_1 - in_2$ ($c_1 = 3.741832 \cdot 10^{-16}$ W·m^2, $c_2 = 1.438786 \cdot 10^{-2}$ m·K) and $\mu = \cos\theta$ ($0 \le \theta \le \pi$). Then the divergence of radiant fluxes at each point of the medium is determined by the following relation [5]:

$$\text{div}\,\mathbf{Q}_r(x) = 2\pi \int_0^\infty \chi_\lambda \left(2B_\lambda\, T(x)) - \int_{-1}^{1} I_\lambda(x, \mu)\, d\mu \right) d\lambda\,. \tag{7}$$

The boundary conditions for the radiation-transfer equation that allow for the reflection and radiation processes on the boundaries of the compound layer differ significantly for the left and right boundaries. This is because the right boundary ($x = H$) transmits inward the radiation $B_\lambda(T_{r.g})$ incident on the boundary from the surroundings and the left boundary (the wall, $x = 0$) is, as a rule, diffusely reflecting and radiating. In that case, the boundary conditions for the incident radiation have the form [6]

$$I_\lambda(0, \mu)\big|_{\mu>0} = \varepsilon_w B_\lambda(T_w) + 2(1 - \varepsilon_w) \int_0^{-1} I_\lambda(0, \mu')\, \mu' d\mu'\,, \qquad I_\lambda(H, \mu)\big|_{\mu<0} = B_\lambda(T_{r.g})\,. \tag{8}$$

Based on the field of the radiation intensities $I_\lambda(x, \mu)$ which is calculated from (6) and (8), the density of the resultant radiative flux from the surface of the compound layer is determined as follows [6]:

$$q_r = \pi \int_0^\infty \left(2 \int_0^1 I_\lambda(H, \mu)\, \mu d\mu - B_\lambda(T_{r.g}) \right) d\lambda\,. \tag{9}$$

Thus, the mathematical model for determination of the heat loss to the surroundings from a wall surface coated with a compound layer which possesses absorbing, emitting, and scattering properties is described by relations (3)–(9). Here the density of the heat-loss flux is the sum of convective loss and radiative loss from the surface, and these losses are determined from (5) and (9) respectively:

$$q = q_{conv} + q_r\,. \tag{10}$$

The algorithm of solution of the problem is as follows:

1. The initial temperature conditions, i.e., T_w, T_a, and $T_{r.g}$, are set.

2. The thermal conductivity of the compound layer λ'_c is set. According to the literature data [7], its mean value is equal to $\lambda'_c = 0.12$ W/(m·K).

3. The spectral optical properties (χ_λ, σ_λ, and ρ_λ) of the compound are calculated (the calculation procedure is given below) over the range of wavelengths $\lambda = 0.3$–100 μm where most of the energy of visible and IR radiation is concentrated. In the same range, the value of ε_w which is known for the majority of materials [8] is set;

4. As a first approximation, it is assumed that $T(x) = T_w$ and $\text{div}\,\mathbf{Q}_r(x) = 0$ at all points of the compound. Next, the densities of the convective q_{0conv} and radiative q_{0r} heat fluxes are calculated from Eqs. (1) and (2) without regard for the compound layer. It is assumed that the flux densities of the radiative and convective heat loss from the compound surface are equal to $q_{conv} = q_{0conv}$ and $q_r = q_{0r}$ respectively.

5. The temperature distribution $T(x)$ in the compound is found from the heat-conduction equation (3) with boundary conditions (2), (4), and (5). The density of the convective-loss flux q_{conv} from the surface is calculated from (5) with account for (2) on the basis of the new temperature distribution in the compound.

6. In the above spectral range, the radiation-transfer equation (6) with boundary conditions (8) is solved, and then $\text{div}\,\mathbf{Q}_r(x)$ and the density of the radiative flux q_r from the compound surface are calculated from (7) and (9) respectively.

7. The accuracy of coincidence of the densities of the convective and radiative fluxes corresponding to two successive iterations is calculated. If it exceeds the assigned one, calculation is repeated from item 5. Otherwise, calculation is completed by obtaining the total heat-flux density q from the compound surface according to (10).

The presented algorithm is closed and enables one to calculate the characteristics of radiative-conductive heat transfer of a wall coated with a compound of hollow ceramic microspheres and a binder with the environment.

Procedure of Solution of the Heat-Conduction Equation in the Compound Layer. At present, there are a great many numerical methods of solving the heat-conduction equation with boundary conditions (4) and (5), of which the most frequently used are the methods of finite elements [9] and finite differences [10]. In the present work, preference is given to the first method.

Without dwelling in detail on the key features of the method itself, we only note that after space discretization we arrive, from the heat-conduction equation, at a system of linear equations for the values of the temperature at the nodes of the calculational grid. Since the vector on the right-hand side of the indicated system depends on the temperature $T(H)$ of the compound surface according to (5), it is necessary to organize the iterative process for successive refinement of the temperature and the density of the convective flux q_{conv}. In this connection, the algorithm of solution of Eq. (3) with boundary conditions (2), (4), and (5) is as follows:

1. As a first approximation, it is supposed that the temperature in the compound layer is uniform and equal to the wall temperature, $T(x) = T_{\text{w}}$.

2. Based on the assigned temperature of the compound surface $T_{\text{c}} = T(H)$, the heat-transfer coefficient α is calculated from (2) and the density of the heat flux on the free surface of the compound q_{conv} is calculated from (5).

3. The coefficients of the system of linear equations with account for the known values of q_{conv} and div $\mathbf{Q}_{\text{r}}(x)$ are calculated and after its solution a new temperature distribution $T(x)$ in the compound is determined.

4. The accuracy of coincidence of the temperature field in the compound for successive iterations is found. If this accuracy exceeds the assigned one, calculation is repeated from Item 2. Otherwise, calculation is completed by obtaining the density of the heat flux q_{conv} from the compound surface in accordance with (2) and (5).

Using the method presented, we calculated the temperature field in the compound layer *without considering* its optical properties. For the temperature and atmospheric conditions described above, the heat loss from the wall surface was determined at $\varepsilon_{\text{c}} = \varepsilon_{\text{w}} = 0.95$ when the wall was coated with the compound layer ($H = 0.5$ mm); the latter was considered to be opaque to radiation (div $\mathbf{Q}_{\text{r}}(x) = 0$). We note that in this case the boundary condition in the form of (1) should be used instead of (5) with replacement of T_{w} by $T(H)$. The calculation showed that under the conditions considered (windless weather, clear or cloudy night sky, $T_{\text{a}} = -15$ to -20^{o}C, $T_{\text{w}} = -10$ to $+10^{\text{o}}$C), the temperature drop over the layer ($\Delta T = T_{\text{w}} - T(H)$) and the relative decrease in heat loss as compared to the uncoated wall ($\Delta q = (1 - q/q_0)\cdot 100\%$) do not exceed 1^{o}C and 4% respectively. These results would be expected, since the coating did not significantly affect either the radiative mechanism of heat transfer that is responsible for the appreciable contribution of the heat loss or the conductive heat transfer due to a very small addition to the thermal resistance of the layer ΔR_{t} ($\Delta R_{\text{t}} = H/\lambda_{\text{c}}' \approx 0.0042\ \text{m}^2\cdot{}^{\text{o}}\text{C/W}$).

Procedure of Solution of the Equation of Radiation Transfer in the Compound Layer. Methods of solution of Eq. (6) with boundary conditions (8) are quite numerous at present: Monte Carlo methods [11], approximations of spherical harmonics [12] and radiative elements [13], the method of characteristics [4], zonal methods [14], etc. Each of the available methods has its own disadvantages and limitations relative to the area of application. One of the last trends in the procedure of solution of the radiation-transfer equation is a combination of the methods of discrete ordinates [15] and finite differences [16, 17] or finite elements [6, 18]. The popularity of such an approach is explained by the relative simplicity of the calculational algorithm and its compatibility with calculational schemes for other mechanisms of energy transfer.

In the present work, we use a new approach [19, 20] to calculation of the problems of radiation transfer that assumes the employment of piecewise analytical (more precisely, formal analytical) solutions for $x_m \le x \le x_{m+1}$ in solving numerically the transfer equation (6) with boundary conditions (8):

$$\mu > 0: \quad I_\lambda(x_{m+1}, \mu) = \exp\left(-\int_{x_m}^{x_{m+1}} \frac{\beta(t)}{\mu}\, dt\right)\left(I_\lambda(x_m, \mu) + \int_{x_m}^{x_{m+1}} \frac{Y(\mu, t)}{\mu} \exp\left(\int_{x_m}^{t} \frac{\beta(\tau)}{\mu}\, d\tau\right) dt\right),$$

$$\mu < 0: \quad I_\lambda(x_m, \mu) = \exp\left(-\int_{x_m}^{x_{m+1}} \frac{\beta(t)}{\mu}\,dt\right)\left(I_\lambda(x_{m+1}, \mu) + \int_{x_{m+1}}^{x_m} \frac{Y(\mu, t)}{\mu} \exp\left(\int_{x_{m+1}}^{t} \frac{\beta(\tau)}{\mu}\,d\tau\right) dt\right), \tag{11}$$

$$\mu = 0: \quad I_\lambda(x_m, \mu) = Y(\mu, x_m)/\beta(x_m), \quad I_\lambda(x_{m+1}, \mu) = Y(\mu, x_{m+1})/\beta(x_{m+1}),$$

where $Y(\mu, x)$ is the right-hand side of Eq. (6) and $\beta(x) = \chi(x) + \sigma(x)$ is the coefficient of total attenuation of the medium. The basis of the method proposed is a combination of the methods of discrete ordinates [15–18] and ray tracing [20]. Radiation intensity is determined along the ray trajectory with account for the optical and geometric properties of the medium and the boundary surface through the use of the piecewise analytical solutions of Eq. (6). For space discretization of the calculational region the concept of the method of finite elements [9, 21] is used, which enables one to describe complex configurations and maintain compatibility with calculational schemes for other mechanisms of energy transfer. As a result of space discretization, we obtain a certain number of discretization elements and nodes (sites) N_{st}, where radiation intensities are thereafter calculated.

Following the method of discrete ordinates we select N_θ directions θ_j of radiation transfer ($\mu_j = \cos\theta_j$, $1 \le j \le N_\theta$) over the range $0 \le \theta \le \pi$ along which the radiation field is calculated. For each of these directions, (6) takes the form

$$\mu_j \frac{\partial}{\partial x} I_j(x) + \beta(x) I_j(x) = Y_j(x), \tag{12}$$

where $I_j(x)$ is the radiation intensity at the point x in the θ_j direction ($1 \le j \le N_\theta$). With account for (11), the solution of (12) in the layer is obtained by superposition of solutions for the portions of the ray path within each element $\Delta_m = x_{m+1} - x_m$. The calculated formulas for (11) within the elements are constructed starting from the characteristics of a concrete problem. The accuracy of interpolation of $\beta(x)$ and $Y_j(x)$ is chosen depending on the extent of inhomogeneity of the medium. For example, in the case of linear interpolation of the indicated quantities over the mth section the recurrence calculated formula for obtaining $I_{m+1,j} = I_j(x_{m+1})$ at $\mu_j > 0$ can be written as follows:

$$I_{m+1,j} = \begin{cases} \left(I_{mj} - \dfrac{Y_{mj}}{\tilde\beta} + \mu_j \dfrac{Y_{m+1,j} - Y_{mj}}{\tilde\beta^2 \Delta_m}\right) \exp\left[-\dfrac{\tilde\beta \Delta_m}{\mu_j}\right] + \dfrac{Y_{m+1,j}}{\tilde\beta} - \mu_j \dfrac{Y_{m+1,j} - Y_{mj}}{\tilde\beta^2 \Delta_j}, & \tilde\beta \Delta_m \ge 10^{-5}; \\ I_{mj} + \dfrac{\Delta_m}{2\mu_j}(Y_{m+1,j} + Y_{mj}), & \tilde\beta \Delta_m < 10^{-5}, \end{cases} \tag{13}$$

where $\tilde\beta = (\beta_{m+1} + \beta_m)/2$. The calculated formula for $\mu_j < 0$ is obtained from (13) by reversal of the sign of Δ_m. To calculate the integral member on the right-hand side of (6) at the mth node of the calculated region for the jth direction, the formula of trapezoids is used. The initial values of the radiation intensity for the recurrence formula (13) are calculated from boundary conditions (8) and, with account for the discretizations performed, have the form

$$I_{1j}\big|_{\mu_j > 0} = \varepsilon_w B_\lambda(T_w) + (1 - \varepsilon_w) \sum_{i=1}^{N_\theta - 1} (I_{1i}\vartheta_i + I_{1,i+1}\vartheta_{i+1}) \left|\mu_{i+1} - \mu_i\right|,$$

$$I_{N_p,j}\big|_{\mu_j < 0} = B_\lambda(T_{r.g}), \quad \text{where} \quad \vartheta_i = \begin{cases} \mu_i, & \mu_i \le 0, \\ 0, & \mu_i > 0. \end{cases} \tag{14}$$

With these relations we can find the field of radiation intensity at all the points of the range calculated for all the directions. However, since the problem is nonlinear (the right-hand side of the transfer equation and the boundary conditions in turn also depend on the intensity), the algorithm of solution is iterative, i.e., the mentioned field is refined successively for each wavelength. The solution algorithm has the following structure:

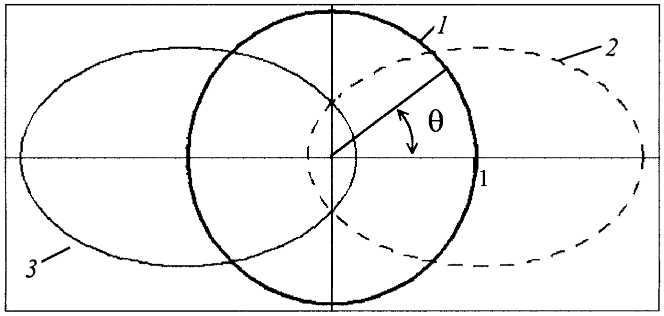

Fig. 2. Model indicatrices of scattering $p(\mu, \mu')$: 1) spherical (b = 0), 2) forward-directed (b = 0.4), and 3) backward-directed (b = –0.4).

1. The initial values of the intensity are assigned. In particular, we can set $I_{ij} = 0$ for all the nodes of the grid and all the directions of radiation propagation.

2. The boundary conditions are calculated according to formulas (14).

3. For each of the selected directions of radiation propagation $j = 1, ..., N_\theta$, the values of I_{ij} are found at each node of the calculated region ($i = 1, ..., N_{st}$). Simultaneously the value of the relative error of coincidence of these values for successive iterations is calculated.

4. If the assigned accuracy is not reached, calculation is repeated from item 2.

As a result of the procedure described, we obtain the basic set I_{ij} for determination of the spectral integral members in the expression for the divergence of radiant fluxes (7) and the density of the resultant radiative flux q_r from the layer surface for the calculated wavelength; in so doing q_r is determined according to (9). Having repeated these calculations for all the considered wavelengths, we find the values of the radiative heat sources div $\mathbf{Q}_r(x)$ and the quantity q_r.

Using the described procedures of solution of the equations of heat transfer and heat conduction, we have solved the problem (3)–(9) on calculation of the characteristics of radiative-conductive heat transfer in the compound layer (H = 0.5 mm) with variation of the optical characteristics of the compound. An analysis of the influence of the optical properties of the compound (χ, σ, and p_λ) on the value of the resultant radiative flux from its free surface was made. To generalized the results, two additional parameters were used: optical thickness of the medium $\tau_2 = \chi H$ characterizing its *absorbing* properties and Schuster criterion $\mathrm{Sc} = \sigma/(\chi + \sigma)$, which is identical to the photon-survival probability used in the literature and determining the contribution of scattering to the process of radiation attenuation by the compound volume. The influence of scattering anisotropy was investigated with the model indicatrix of scattering of Henyey–Greenstein [22]:

$$p(\mu, \mu') = \frac{1 - b^2}{\left(1 + b^2 - 2b\left[\mu\mu' + \sqrt{(1-\mu^2)(1-\mu'^2)}\right]\right)^{3/2}}, \tag{15}$$

where $-1 < b < 1$ is the asymmetry factor and $\cos\theta = \mu\mu' + \sqrt{(1-\mu^2)(1-\mu'^2)}$. Figure 2 plots the indicatrices for isotropic and predominantly forward- and backward-directed scattering which correspond to the calculation results given below.

A comprehensive investigation of the influence of the optical properties of an absorbing, radiating, and scattering two-phase medium and its boundaries on the characteristics of radiative energy transfer can be found in [6, 18, 23]. Because of this, in what follows we dwell on only the basic results of mathematical modeling that are significant for the problem studied in this work. Calculation shows that with increase in the fraction of scattering processes the density of the radiation flux from the compound surface substantially decreases for the spherical and backward-directed indicatrices of scattering and increases for the forward-directed indicatrix. For a strongly scattering compound deposited on a wall of high emissivity (Fig. 3a) an increase in the optical thickness of the compound leads to a nonlinear decrease in the flux density of the radiative and, consequently, total loss. If the self-emissivity of the wall is low (Fig. 3b), the indicated effect can not appear at all or even be inverted, i.e., the radiative flux will increase. We note that

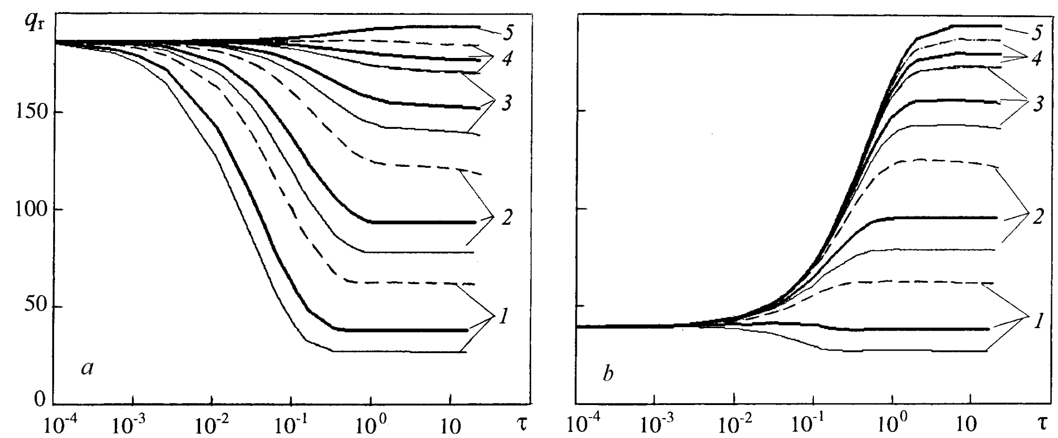

Fig. 3. Change in the radiative flux from the compound surface under a clear night sky as a function of the optical properties of the compound for ε_w = 0.95 (a) and 0.2 (b), $T_w = 0^oC$, and $T_a = -20^oC$: 1) Sc = 0.98, 2) 0.9, 3) 0.6, 4) 0.3, and 5) 0. Different types of lines correspond to different indicatrices of scattering in Fig. 2. q_r, W/m^2; τ is the dimensionless quantity.

for the forward-directed indicatrix of scattering the radiative flux from the compound surface decreases more slowly than that for the backward-directed indicatrix, since in the latter case the layer possesses a higher reflectivity (Fig. 3). Of importance is also the fact that the radiative flux from the surface of a painted wall reaches a constant value even for an optical thickness of the coating of the order of 0.2 (Fig. 3a).

The presented results show that the optical properties of semitransparent heterogeneous media including compounds of hollow ceramic microspheres substantially affect the radiative flux. This suggests the expediency of the development and employment of such media for both heat-reflecting and nonreflecting coatings where the latter are necessary.

Procedure of Calculation of the Optical Characteristics of the Compound Layer. The process of scattering of radiation is the most intense in optically inhomogeneous media when the gradients of refractive index are sufficiently large. In most cases these gradients arise when particles with a refractive index different from that of the media are present in the scattering volume.

The scattering of IR (thermal) radiation (0.7–75 μm) on spheres with a diameter of 0.01–100 μm can substantially change the heat transfer in the layer. As has been noted above, in this case correct description of the processes of radiative heat transfer necessitates the additional use of the integro-differential equation of radiation transfer that includes the optical characteristics of an elementary volume of the layer, namely, σ_λ, χ_λ, and $p_\lambda(\mu, \mu')$. These characteristics depend on the dimension of the spheres (in the simplest case on the radius a), the distance between the spheres d, the complex refractive indices of the medium and the spheres, and the wavelength of the scattered radiation. Moreover, it is necessary to allow for the dispersion of the refractive index, i.e., its dependence on the wavelength of the incident radiation. In this work, we have used the refractive indices of glass particles in air and of air cavities in glass for the IR range that were taken from [24].

The problem of scattering of light on a sphere was analytically solved early in the 20th century. For this case, the solution of the Maxwell equations referred to as the Mie solution was obtained in the form of infinite convergent series (see, for example, [25]). The use of this solution for description of radiation scattering by a certain medium containing inclusions (particles) is possible only if the scattering on the particles is independent. This implies that the distance between the particles must be considerably larger than the size of them and the wavelength.

This assumption holds for most optical problems. The composite coating considered in this work is effective only if the volume concentration of microspheres is sufficiently high (~40–50%), which results in a failure of the conditions of independent scattering of radiation. Therefore, in this case the use of results of the classical Mie theory can lead to significant mistakes in calculating the corresponding characteristics. We note that in investigating close packings of particles one should also use care in employment of the radiation-transfer equation. For example, this equation cannot be used in most cases of treating problems related to an analysis of the radiation structure [26]. If we are dealing with the integral (over the angle) characteristics of the light field, this equation can be used with correct determination of the parameters ε, σ, and p_λ [26].

In [27], the problem of radiation scattering by two spherical particles placed close to each other has been solved. According to [27], the functions of radiation scattering in the medium with a refractive index m_b that are of interest to us are as follows:

$$S_1(\theta) = \sum_{n=1}^{\infty} \frac{2n+1}{n(n+1)} [M_n \pi_n(\cos\theta) + N_n \tau_n(\cos\theta)],$$

$$S_2(\theta) = \sum_{n=1}^{\infty} \frac{2n+1}{n(n+1)} [M_n \tau_n(\cos\theta) + N_n \pi_n(\cos\theta)], \tag{16}$$

where the partial coefficients are determined by the expressions

$$M_n = \frac{\zeta_n'(kd)[\psi_n(ka)\psi_n'(m_b ka) - m_b \psi_n(m_b ka)\psi_n'(ka)]}{kd[\zeta_n(ka)\psi_n'(m_b ka) - m_b \psi_n(m_b ka)\zeta_n'(ka)]},$$

$$N_n = \frac{\zeta_n(kd)[\psi_n(ka)\psi_n'(m_b ka)m_b - \psi_n(m_b ka)\psi_n'(ka)]}{kd[\zeta_n(ka)\psi_n'(m_b ka)m_b - \psi_n(m_b ka)\zeta_n'(ka)]}. \tag{17}$$

Here $k = 2\pi m_b/\lambda$, $\pi_n(\cos\theta) = \frac{1}{\sin\theta} P_n(\cos\theta)$, $\tau_n(\cos\theta) = \frac{d}{d\theta} P_n(\cos\theta)$, and $P_n(\cos\theta)$ are the Legendre polynomials of the real argument and ψ_n and ζ_n are the Riccati–Bessel functions (primes denote their derivatives).

Expressions (17) differ from the classical Mie solution by the factors $\zeta_n'(kd)$ and $\zeta_n(kd)$ accounting for the sphericity of scattered waves, i.e., in fact, the influence of a close packing of particles on the scattering process.

According to [25], the differential scattering cross section for the particles in a unit solid angle for a unit unpolarized incident flux of radiation has the form

$$d\sigma_s(\theta) = \frac{1}{2|k|^2}\left(|S_1|^2 + |S_2|^2\right) d\omega. \tag{18}$$

Integrating (18) over the entire solid angle 4π, we can obtain the scattering coefficient for an individual particle σ_s:

$$\sigma_s = \int_{4\pi} d\sigma_s(\theta) = \frac{1}{2|k|^2} \int_{4\pi} \left(|S_1|^2 + |S_2|^2\right) d\omega. \tag{19}$$

This coefficient related to the geometric cross section of a particle determines the efficiency factor of scattering [27] with account for the distance between the particles:

$$K_\sigma = \frac{\sigma_s}{\pi a^2} = \frac{2S'}{|\rho|^2} \sum_{n=1}^{\infty} (2n+1)\left[|M_n|^2 + |N_n^2|\right], \tag{20}$$

where $\rho = ka = 2\pi m_b a/\lambda$, $\rho' = \pi d/\lambda$, and $S' = 1 - |\rho|/|\rho'|$ (for the Mie solution we have $S' = 1$). Next, according to the optical theorem of attenuation, we can obtain the factor of radiation attenuation by a particle with consideration for the distance between the particles:

$$K_\beta = \frac{2S'}{|x|^2} \sum_{n=1}^{\infty} (2n+1)\,\mathrm{Re}\left\{M_n + N_n\right\} . \qquad (21)$$

The absorption factor is equal to the difference of the attenuation and scattering factors:

$$K_\chi = K_\beta - K_\sigma . \qquad (22)$$

The last of the necessary characteristics is the scattering indicatrix normalized to the total solid angle 4π, which can be found in the following way:

$$p\,(\mu, \mu') = \frac{2}{|\rho|^2 K_\sigma} \left[|S_1(\theta)|^2 + |S_2(\theta)|^2 \right] . \qquad (23)$$

After determination of the absorption and scattering coefficients and the indicatrix of radiation scattering for an individual particle, the optical characteristics of the compound that are of interest to us are obtained as follows [8, 28]:

a) for a monodisperse system of particles with radius a and concentration N_0, the absorption and scattering coefficients are equal respectively to

$$\chi = \pi a^2\, K_\chi\,(m, \lambda, a, d)\, N_0 , \qquad (24)$$

$$\sigma = \pi a^2\, K_\sigma\,(m, \lambda, a, d)\, N_0 , \qquad (25)$$

and the scattering indicatrix is determined by expression (23);

b) for a polydisperse system, the size distribution function of particles is brought into consideration instead of the size of an individual particle. All the radiative characteristics of such a system must be averaged over this distribution function.

Calculation of the Heat-Protection Properties of the "Ceramic Microspheres–Binder" Compound. Let us calculate, based on the proposed mathematical model, the total heat flux from the wall surface (ε_w = 0.95) covered with the heat-protection coating "ceramic microspheres–binder" for the above-indicated temperature and atmospheric conditions with the following parameters of the compound: mean diameter of microspheres 35 μm, their concentration in the compound layer $N_0 = 2.5 \cdot 10^{12}$ m^{-3}, and mean distance between them d = 40 μm.

The calculation has shown (Fig. 4) that the optical properties of the compound and consequently the density of the radiative flux from its surface depend on the radiation wavelength. This is confirmed by the results presented in Fig. 5, which illustrates the spectral densities of the radiative flux from the compound surface under a clear night sky as compared to the same quantities for a "bare" wall with a practically constant emissivity in the considered spectral range. To simplify the analysis of the results for the compound, we introduce the concept of the effective emissivity, which is equal to the ratio of the integral radiative flux from the compound surface (9) to the integral radiative flux from the surface of the ideal black body (1):

$$\varepsilon_c = \frac{q_r}{\sigma_0\,(T_w^4 - T_{r.g}^4)} . \qquad (26)$$

The effective emissivity of the compound is a complex function depending on the geometric thickness of the compound layer, the microsphere dimension and concentration, the temperature and emissivity of the wall on which the compound is deposited, and the conditions of irradiation of the compound, i.e., the state of the environment: air temperature, clouds, presence of other radiating objects (the sun, nearby buildings, and so on). For example, for the results presented in Fig. 5 the effective emissivity is approximately equal to 0.4, and for a cloudy sky (all other things being the same) it decreases and becomes equal to 0.3. This effective characteristic also diminishes with decrease in the tem-

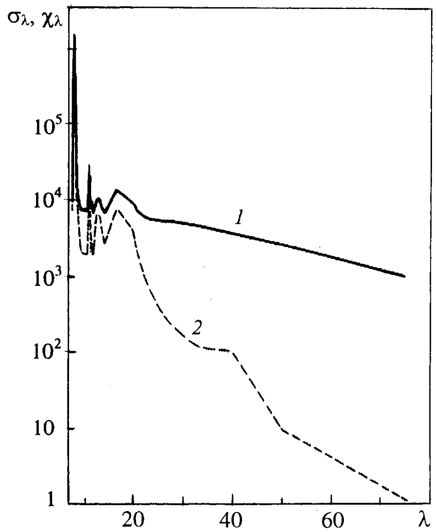

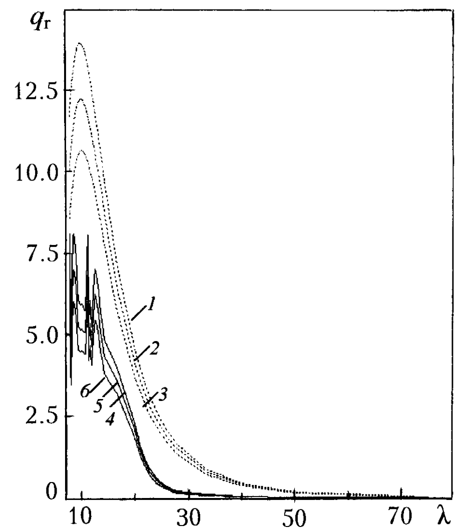

Fig. 4. Spectral coefficients of absorption σ_λ (1) and scattering χ_λ (2) of the "ceramic microspheres–binder" compound. σ_λ, m^{-1}; χ_λ, m^{-1}; λ, μm.

Fig. 5. Spectral densities of the radiation flux from the surface of the "bare" wall (1–3) and the wall coated with the compound (4–6) on a clear windless night for T_a = –20^{o}C and T_w = 0^{o}C (1 and 4); –5^{o}C (2 and 5); –10^{o}C (3 and 6). q_r, W/(m^2·μm); λ, μm.

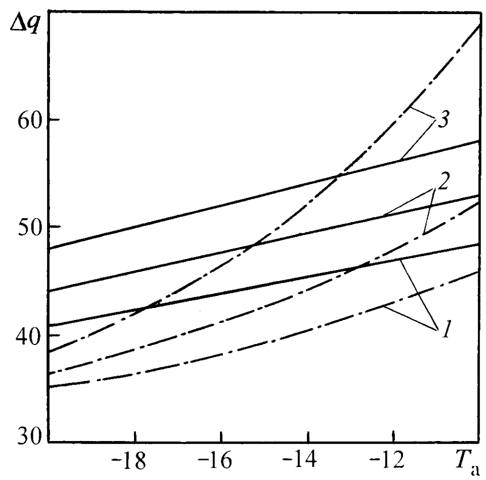

Fig. 6. Relative decrease in the heat loss from the wall surface (ε_w = 0.95) coated with the "ceramic microspheres–binder" compound as compared to the "bare" wall in windless weather under a clear (solid lines) and cloudy (dashed lines) night sky for different temperatures of the wall surface: 1) T_w = 0^{o}C; 2) –5^{o}C; 3) –10^{o}C. Δq, %; T_a, ^{o}C.

perature drop between the wall surface and the surrounding air. Thus, the calculations have shown that under the above conditions the investigated composite coating can decrease the total heat loss by more than 40% (Fig. 6).

Experiment. To test the applicability of the above mathematical model of calculating the heat-insulation properties of the "ceramic microspheres–binder" compound, a set of experiments has been performed at the Scientific-Research Institute of Building Materials (Minsk).

First of all, the contribution of thermal radiation to the total heat loss from the wall surface was experimentally determined. On the external surface of the north wall of a building, two meters of the heat-flux density were symmetrically secured, on one of which an aluminum foil 0.1 mm thick was tightly glued. On the night of June 29

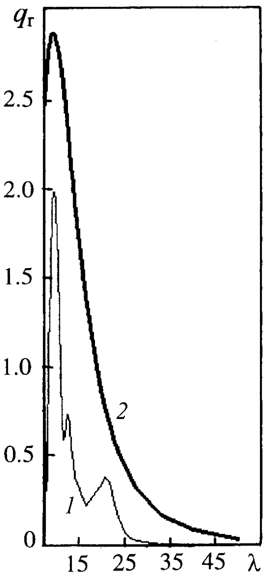

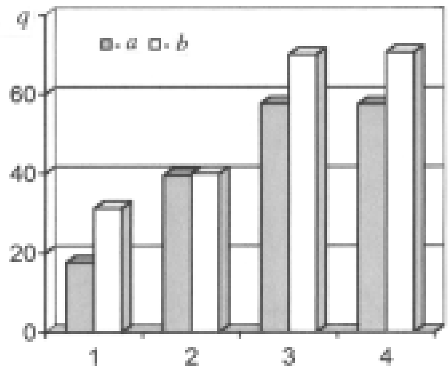

Fig. 7. Spectral density of the radiative flux from the wall surface: 1) surface painted with the compound; 2) nonpainted surface. q_r, W/(m^2·μm); λ, μm.

Fig. 8. Structure and values of the heat loss from the surface of the wall fragment under the conditions of a climatic chamber: 1) radiative loss (calculation); 2) convective loss (calculation); total heat loss: 3) calculation; 4) experiment; a) painted wall; b) nonpainted wall. q, W/m^2.

to 30, the readings of the sensors of the heat flux (calorimeters) and the temperatures of the wall and the surrounding air were recorded. The measurement results were as follows: a) the mean wall temperature over the period from 21.00 to 5.00 was equal to T_w = 12.5^{o}C; b) the mean temperature of the outer air over the same period was T_a = 11.5^{o}C; c) the mean densities of the heat flux from the foil-clad and non-foil-clad calorimeters were equal to q_f = 13.5 W/m^2 and q_{nf} = 39.1 W/m^2 respectively. As is seen from the experimental results, the heat loss became practically three times smaller and, since the intrinsic thermal resistance of the aluminum foil is negligibly small, it may be concluded that the conditions of heat exchange of the wall surface with the surrounding space changed in this case. The given experimental situation was simulated numerically using the developed mathematical model. Here the emissivity of the aluminum foil was chosen to be equal to ε = 0.25. The simulation results (q_f = 13.5 W/m^2, q_{nf} = 38.7 W/m^2) practically coincided with experimental ones.

In the second part of the experimental investigation, in a climatic chamber we measured the density of the heat flux from the surface of the wall fragment, half of which was painted with the heat-protection compound. The physical conditions of the experiment were as follows: a) the air temperature in the cold part of the climatic chamber was held at T_a = -27 ± 1^oC; b) the mean temperatures of the painted and nonpainted wall surfaces were equal to $T_{w.p}$ = -16.4^oC and $T_{w.np}$ = -18.2^oC respectively. The mean densities of the heat flux from the painted and nonpainted wall surfaces turned out to be equal to q_p = 57.5 W/m^2 and q_{np} = 70.6 W/m^2 respectively. To calculate the heat-flux densities according to the mathematical model, we introduced additional limitations: a) the hemispherical emissivity of the nonpainted surface of the wall was taken equal to ε_w = 0.95; b) it was assumed that $T_{r.g} = T_a$, as the climatic chamber is an closed space; c) the volume concentration of microspheres in the compound was assigned equal to 50%. The calculation results presented in Figs. 7 and 8 agree well with the experimental data: the error is no higher than 3%. The calculation showed (Fig. 7) that under the mentioned thermophysical experimental conditions, $\varepsilon_c \approx 0.3$, which is a result of a substantial decrease in the density of the radiative flux from the wall surface.

It should be noted that all the more substantial decrease in the radiative flux is observed in testing of the coating under full-scale conditions when we have radiative energy exchange with the sky. Evaluation of the error introduced by the climatic chamber and determined by the difference of the sky temperature (T_r = -73^oC = 200 K) from the temperature of the cold part of the climatic chamber has shown that under full-scale conditions the investigated coating results in a decrease of approximately 40% in the heat loss for the indicated climatic conditions.

In closing, we can note that a decrease in the volume concentration of ceramic microspheres in the compound leads to a decrease in the heat-protection properties of the coating, and even at concentrations lower than 15% the coating practically ceases to affect the structure and the value of the heat loss, turning to an ordinary paint.

CONCLUSIONS

1. Coatings that are a compound of a binder and hollow ceramic microspheres are an efficient means of additional heat protection of enclosing structures.

2. The heat-protection effect of the composite coating "ceramic microspheres–binder," by virtue of the physical principle of its operation, substantially depends quantitatively on the optical properties of the substrate (wall) and the environment and on the temperature regime of operation (in some situations, the heat-protection effect can be inverted).

3. The developed mathematical model and the corresponding computer codes adequately reflect the actual process of heat transfer and can be used for calculation of the heat-protection properties of coatings that are compounds of a binder and hollow ceramic microspheres.

The authors are grateful to Corresponding Member of the National Academy of Sciences of Belarus N. V. Pavlyukevich for fruitful discussion in the fulfillment of the work.

This work was carried out with support from INTAS (grant 2000-652).

NOTATION

T, temperature; ε, hemispherical emissivity; q, heat-flux density; H, thickness of the compound layer; λ', thermal conductivity; a', thermal diffusivity; g, gravitational acceleration; λ, wavelength of electromagnetic radiation; N, number of nodes; θ, angle between the direction of propagation of the ray and the $0x$ axis; $\mu = \cos\theta$; θ', angle between the direction of scattering of the ray and the $0x$ axis; $\mu' = \cos\theta'$; x, spatial coordinate; $I_\lambda(x, \mu)$, spectral intensity of radiation at a wavelength λ at the point x in the θ direction; χ, coefficient of absorption of radiation in the compound; σ, coefficient of scattering of radiation in the compound; $p_\lambda(\mu, \mu')$, indicatrix of scattering of radiation; m and n, refractive indices; K_χ, K_β, and K_σ, coefficients of radiation absorption, attenuation, and scattering, respectively, by a particle; Sc, Schuster criterion; α, coefficient of convective heat transfer from the surface; L, wall height; $\mathbf{Q}_r$, density of the radiative fluxes; β, coefficient of total attenuation of the medium; τ, optical thickness; ρ, diffraction parameter of the microspheres; b, asymmetry factor of the model indicatrix of scattering. Subscripts: w, wall; r, radiative; conv, convective; a, atmosphere; c, compound; b, binder; g, ground surface; f, foil-clad; nf, non-foil-clad; p, painted; np, nonpainted; s, scattering; st, site (node); t, thermal; V, volumetric; 0, absence of the compound layer.

REFERENCES

1. F. Kreith and W. Z. Black, *Basic Heat Transfer* [Russian translation], Moscow (1983).
2. O. G. Martynenko and Yu. A. Sokovishin, *Free-Convective Heat Transfer* [in Russian], Minsk (1982).
3. A. V. Luikov, *Heat and Mass Transfer* [in Russian], Moscow (1978).
4. K. S. Adzerikho, E. F. Nogotov, and V. P. Trofimov, *Radiative Heat Transfer in Two-Phase Media* [in Russian], Minsk (1987).
5. W. A. Fiveland, *J. Heat Transfer*, **106**, 699–706 (1984).
6. M. L. German, *Influence of the Optical Properties of Two-Phase Medium and a Boundary Surface on Radiative Heat Transfer in Furnace Chambers*, Candidate's Dissertation (in Physics and Mathematics), Minsk (1993).
7. V. V. Budov, *Steklo Keramika*, No. 7, 7–11 (1994).
8. A. G. Blokh, Yu. A. Zhuravlev, and L. N. Ryzhkov, *Radiative Heat Transfer. Handbook* [in Russian], Moscow (1991).
9. T. Shih, *Numerical Heat Transfer* [Russian translation], Moscow (1988).
10. E. F. Nogotov, *Application of Numerical Heat Transfer*, McGraw-Hill, New York (1978).
11. R. Siegel and J. R. Howell, *Thermal Radiation Heat Transfer* [Russian translation], Moscow (1975), pp. 795–804.

12. M. Menguc and R. Viskanta, *JQSRT*, **35**, 533–549 (1985).
13. S. Maruyama and T. Aihara, in: *Proc. 1st Int. Symp. on Radiation Transfer*, Kusadasi, Turkey (1995), pp. 153–167.
14. H. C. Hottel and A. F. Sarofim, *Radiative Transfer*, McGraw-Hill, New York (1967).
15. S. Chandrasekhar, *Radiative Transfer*, New York (1960).
16. W. A. Fiveland, *J. Heat Transfer*, **109**, 809–812 (1987).
17. J. S. Truelove, *JQSRT*, **39**, 27–31 (1988).
18. M. L. German, V. P. Nekrasov, and E. F. Nogotov, *Dokl. Akad. Nauk Belarusi*, **40**, No. 3, 122–126 (1996).
19. E. A. German, M. L. German, V. P. Nekrasov, and E. F. Nogotov, *Inzh.-Fiz. Zh.*, **69**, No. 6, 1014–1020 (1996).
20. M. L. German, V. P. Nekrasov, and E. F. Nogotov, *Dokl. Akad. Nauk Belarusi*, **42**, No. 1, 67–73 (1998).
21. M. L. German, P. M. Kolesnikov, and E. F. Nogotov, in: *Proc. Int. Conf. "Thermal Physics-98"* [in Russian], Obninsk (1998), pp. 301–308.
22. K. N. Liou, *An Introduction to Atmospheric Radiation* [Russian translation], Leningrad (1984).
23. O. G. Martynenko, M. L. German, V. P. Nekrasov, and E. F. Nogotov, *Int. J. Heat Mass Transfer*, **41**, No. 17, 2697–2704 (1998).
24. V. M. Zolotarev, V. N. Morozov, and E. V. Smirnova, *Optical Constants of Natural and Engineering Media* [in Russian], Leningrad (1984).
25. H. C. van de Hulst, *Light Scattering by Small Particles* [Russian translation], Moscow (1961).
26. A. P. Ivanov and V. G. Danilyuk, *Opt. Spektrosk.*, **42**, No. 4, 739–746 (1977).
27. T. P. Ryzhkova and L. N. Ryzhkov, *Prom. Teploénerget.*, **1**, No. 3, 26–34 (1983).
28. D. Deirmendjian, *Electromagnetic Scattering on Spherical Polydispersions* [in Russian], Moscow (1971).